

## Parameter Estimation of *Paramecium* Model using Real-coded Genetic Algorithm

Akira Hirano<sup>†</sup>, Zu Soh<sup>†</sup>, Toshio Tsuji<sup>†</sup>, Noboru Takiguchi<sup>††</sup>, and Hisao Ohtake<sup>†††</sup>

<sup>†</sup>Graduate School of Engineering, Hiroshima Univ., Hiroshima 739-8527, Japan

<sup>††</sup>Graduate School of Advanced Sciences of Matter, Hiroshima Univ., Hiroshima 739-8530, Japan

<sup>†††</sup>Graduate School of Engineering, Osaka Univ., Osaka 565-0871, Japan

### Abstract

In previous studies [5, 7], we proposed the computer model of *Paramecium*, *Virtual Paramecium*, based on biological knowledge. The model can approximately realize the membrane potential change for chemical stimuli and mechanical stimuli. The parameters included in the model were determined based on the results of experiments with the actual organisms, although some parameters could include estimated errors. The simulated membrane potential changes by the model, however, showed the different property of time variation from the ones of the living organism.

In this paper, we propose an estimation method of the model parameters included in the *Virtual Paramecium* using a real-coded genetic algorithm. The method automatically searches the model parameters that can approximately realize the membrane potential change in the actual *Paramecium*.

## 1 Introduction

Protozoan shows specific reaction to various stimuli in the environment. For example, *Paramecium* swims to the cathode when the DC electrical field is applied in the environment; this mechanism is called electro-taxis. Recently, a number of studies have proposed to utilize *Paramecium* as a kind of micro-machine using the electro-taxis [1]-[4]. Itoh collected the behavioral data of *Paramecium* to an electrical stimulus, and proposed a control law based on these statistical data [2]. In addition, Ogawa *et al.* developed a tracking system which can keep *Paramecium* under the microscopical field to control its behavior [4]. Further, they constructed a computer model to simulate the electro-taxis of *Paramecium* based on experimental results [3]. However, experiments to collect these data are extremely time consuming. Moreover, the control law based on the behavioral experimental data cannot

always be applied to the actual control because the intracellular characteristics of *Paramecium* are determined corresponding to the various ion concentrations in environments. Therefore, if a computer model can be constructed to realize the behavior based on the intracellular changes corresponding to the environmental conditions, an effective control law of *Paramecium* could be derived.

We have proposed the calculation model of membrane potential change of *Paramecium* [5] based on the Hodgkin-Huxley model, which could explain the generation and propagation of action potentials in the squid giant axon [6]. Further, we developed the artificial life model, "*Virtual Paramecium*," which was able to realize the behavior based on the results of the internal processing for stimuli [7]. The parameters included in the model were determined based on the results of experiments with the actual organisms, although some parameters could include estimated errors. The simulated membrane potential changes by the model, however, showed the different property of time variation from the ones of the living organism.

Various kinds of nonlinear optimization methods have been proposed to determine the parameters included in the physical models. In several previous studies [8]-[10], it was reported that the genetic algorithm method is an effective method to determine the model parameter values of organisms. In this paper, we propose an estimation method of the model parameters included in the *Virtual Paramecium* using a real-coded genetic algorithm. In addition, we report on the results that the estimated model parameters by the proposed method are able to realize the time variation of membrane potential change similar to that of the living organism.

This paper is organized as follows: In Section 2, the calculation model of the membrane potential change of *Paramecium* is described. In Section 3, the estimation method of the model parameters to realize the membrane potential change of actual organism is pro-

posed. In Section 4, the effectiveness of the estimated parameters in Section 3 is verified through a series of computer simulations.

## 2 Information processing model of *Paramecium*

### 2.1 The mechanism of the membrane potential change [11]

*Paramecium* processes information by electrophysiological phenomena. Ion channels and ion pumps that reside in the membrane play an important role in maintaining the ionic connection between the interior and the exterior of the cell. In a standard salt solution, the membrane potential is maintained at approximately 20 mV lower than that of the external environment when no stimuli are presented from the environment. When *Paramecium* receives a stimulus, the ion channels open, and ionic flow occurs across the interior and the exterior of the cell. First, the voltage-sensitive  $\text{Ca}^{2+}$  channel opens, and the membrane potential is depolarized by the  $\text{Ca}^{2+}$  flow into the cell. With a few millisecond delay, the voltage-sensitive  $\text{K}^+$  channel opens responding to the membrane potential change opens, and the membrane potential is hyperpolarized by the  $\text{K}^+$  flows outside the cell. From this mechanism, the spike-like potential change occurs. In the next section, we explain the calculation model of the membrane potential change of *Paramecium*.

### 2.2 The calculation model of the membrane potential change

The electrical characteristics of the cell membrane can be expressed by the electric circuit as shown in Figure 1 [5]. Figure 1 illustrates the relationship between the change in membrane potential and ionic flow into a cell, in which the ion channels are affected by the membrane potential. In the figure, the cell membrane, the ion channels and the flow of ion are considered as a condenser, active resistive elements and electric currents, respectively.

First, the electrical characteristics of *Paramecium* are modeled based on a Hodgkin-Huxley type equation [6] as follows [5]:

$$\dot{V}(t) = \frac{1}{C_m} [I(t) - I_{\text{Ca}}(t, V) - I_{\text{K}}(t, V) - I_{\text{leak}}(t, V)], \quad (1)$$

where  $V(t)$  is the membrane potential,  $I(t)$  the stimulated current, and  $C_m$  the membrane capacity. The  $\text{Ca}^{2+}$  current  $I_{\text{Ca}}(t, V)$ , the  $\text{K}^+$  current  $I_{\text{K}}(t, V)$ , and

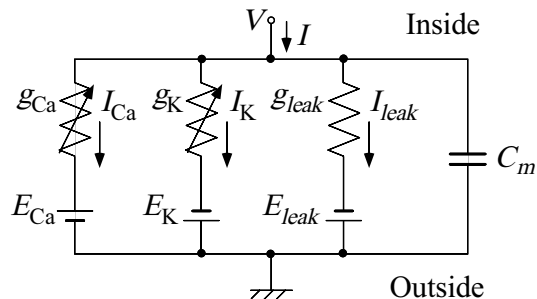


Figure 1: An electric circuit model for the *Paramecium*.

the leakage current  $I_{\text{leak}}(t, V)$  are given by the following equations [5]:

$$I_{\text{Ca}}(t, V) = \bar{g}_{\text{Ca}} m^5 \{1 - (1 - h)^5\} (V(t) - E_{\text{Ca}}), \quad (2)$$

$$I_{\text{K}}(t, V) = \bar{g}_{\text{K}} n (V(t) - E_{\text{K}}), \quad (3)$$

$$I_{\text{leak}}(t, V) = g_{\text{leak}} (V(t) - E_{\text{leak}}), \quad (4)$$

where  $\bar{g}_{\text{Ca}}$ ,  $\bar{g}_{\text{K}}$ , and  $g_{\text{leak}}$  are the maximum values of the ion conductance for  $\text{Ca}^{2+}$ ,  $\text{K}^+$  and leakage ion channels, respectively. Equilibrium potentials for  $\text{Ca}^{2+}$ ,  $\text{K}^+$  and leakage ions are expressed as  $E_{\text{Ca}}$ ,  $E_{\text{K}}$  and  $E_{\text{leak}}$ , respectively. Also,  $m$ ,  $h$  and  $n$  are the activation probabilities of each ion channel [5, 6]. For example, the change of  $m$  from 0 to 1 means the increasing of the activation probability in  $\text{Ca}^{2+}$  channels. In addition, the change of  $n$  from 0 to 1 means the increasing of the activation probability in  $\text{K}^+$  channels. In Eqs. (2) to (4), the values of  $m$ ,  $h$  and  $n$  were decided based on Reference [12].

Activation probabilities,  $x \in \{m, h, n\}$ , of each channel are calculated based on the Hodgkin-Huxley equations [6] as follows [13]:

$$\dot{m}(t, V) = \alpha_m(V) \cdot (1 - m(t, V)) - \beta_m(V) \cdot m(t, V), \quad (5)$$

$$\dot{h}(t, V) = \alpha_h(V) \cdot (1 - h(t, V)) - \beta_h(V) \cdot h(t, V), \quad (6)$$

$$\dot{n}(t, V) = \alpha_n(V) \cdot (1 - n(t, V)) - \beta_n(V) \cdot n(t, V), \quad (7)$$

where  $\alpha_x$ ,  $\beta_x$  ( $x \in m, h, n$ ) are the rate constant of ion channel [6], and its characteristics is nonlinear for the membrane potential  $V$ .

### 2.3 State transition model of ion channels

In this paper, Eqs. (5) to (7) are expressed as the following equations to discuss the time characteristics of ion channels [14]:

$$\dot{x} = \frac{1}{\tau_x(V)} (x^\infty(V) - x(V)) \quad (x \in m, h, n), \quad (8)$$

$$\tau_x(V) = \frac{1}{\alpha_x(V) + \beta_x(V)} \quad (x \in m, h, n), \quad (9)$$

$$x^\infty(V) = \frac{\alpha_x(V)}{\alpha_x(V) + \beta_x(V)} \quad (x \in m, h, n), \quad (10)$$

where  $x^\infty(V)$  is the steady-state characteristics of the gate parameters, and  $\tau_x$  the time constant. The values are calculated from the result of the voltage-clamp experiment with actual organism [15].

$\alpha_x$  and  $\beta_x$  ( $x \in \{m, h, n\}$ ) in Eqs. (9) and (10) are expressed as the following equations:

$$\alpha_m(V) = \frac{p_0(V + p_1)}{1 - \exp\left[-\frac{V + p_1}{p_2}\right]}, \quad (11)$$

$$\beta_m(V) = p_3 \exp\left[-\frac{V + p_4}{p_5}\right], \quad (12)$$

$$\alpha_h(V) = p_6 \exp\left[-\frac{V + p_7}{p_8}\right], \quad (13)$$

$$\beta_h(V) = \frac{p_9}{1 + \exp\left[-\frac{V + p_{10}}{p_{11}}\right]}, \quad (14)$$

$$\alpha_n(V) = \frac{p_{12}(V - p_{13})}{1 - \exp\left[-\frac{V - p_{13}}{p_{14}}\right]}, \quad (15)$$

$$\beta_n(V) = p_{15} \exp\left[-\frac{V - p_{16}}{p_{17}}\right], \quad (16)$$

where  $p_n$  ( $n = 1, 2, \dots, 17$ ) is constants that determine the characteristics of  $\alpha_x$  and  $\beta_x$  ( $x \in \{m, h, n\}$ ). The value of  $p_n$  is determined from the voltage-clamp experiment with actual organism. In the next section, the values of  $\alpha_x$  and  $\beta_x$  ( $x \in \{m, h, n\}$ ) are determined by a real-coded GA.

### 3 Parameter Estimation by a real-coded GA

#### 3.1 The estimation method of parameters

In this paper,  $p_n$  ( $n = 1, 2, \dots, 17$ ),  $\bar{g}_{Ca}$  and  $\bar{g}_K$  are estimated by the real-coded GA. Then,  $p_n$  ( $n = 1, 2, \dots, 17$ ) are used to determine the characteristics of  $\alpha_x$  and  $\beta_x$  ( $x \in \{m, h, n\}$ ). The procedure used in this paper is described below;

##### Step 0 : Initialization

First, the maximum generation number  $G_{\max}$  and the number of individuals  $M$  are set. Then, the initial individuals are prepared as follows. The individuals are coded as the combination of  $p_n$  ( $n = 1, 2, \dots, 17$ ),  $\bar{g}_{Ca}$  and  $\bar{g}_K$ . The initial value of each parameter is determined randomly within

the neighborhood domain of the estimated parameter values by the experiment with actual organisms [5]. The initial values of  $\bar{g}_{Ca}$  and  $\bar{g}_K$  are determined randomly within four to six times of the  $g_{\text{leak}}$  value based on Reference [5].

##### Step 1 : Evaluation

The current stimuli simulation is carried out for each individual. Then, the root mean square error of the actual membrane potential and the simulated result,  $F_m$ , is calculated by the following equation:

$$F_m = \frac{1}{T} \sum_{s=1}^N \int_0^T \sqrt{(D_s(t) - O_{(m,s)}(t))^2} dt, \quad (17)$$

where  $D_s(t)$  is the membrane potential change of actual *Paramecium* for the current stimuli used  $I_s$ ,  $O_{(m,s)}(t)$  the simulated membrane potential, the suffix  $m$  the individual number,  $T$  the simulation time,  $N$  the number of the current stimuli  $I_s$ .

##### Step 2 : Selection

Each individuals is arranged in order of  $F_m$ . Then,  $\gamma_e$  individuals with superior fitness values are selected and saved in the nest generation.

##### Step 3 : Crossover

$\gamma_c$  individuals are generated by the BLX- $\alpha$  method [16], where  $\gamma_c = N - \gamma_e$ . For generation of each  $\gamma_c$  individuals are chosen from among the superior  $\gamma_e$  individuals.

##### Step 4 : Mutation

Randomly choose  $\gamma_m$  individuals from among  $\gamma_c$  individuals given by the crossover at random, and replace them with randomly determined values within the initial domain.

##### Step 5 : Update

The procedure from steps 1-4 is repeated for the maximum generation number  $G_{\max}$ .

### 3.2 Non-search parameters set

The non-search parameters by the GA were set based on the research data in biological field. The membrane capacitance  $C_m$  included in Eq. (1) was determined based on Reference [17] as  $C_m = 1 \mu\text{F}$ . The equilibrium potentials  $E_{Ca}$ ,  $E_K$  and the resting membrane potential  $V(0)$  were set as follow :  $E_{Ca} = 120 \text{ mV}$ ,  $E_K = -40 \text{ mV}$ ,  $V(0) = -21.0 \text{ mV}$ , on the assumption that the standard solution environment.

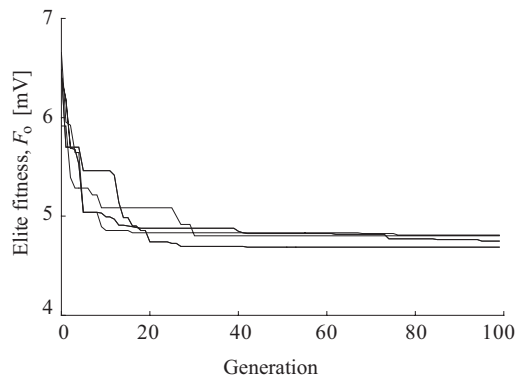


Figure 2: Evolution of the elite fitness.

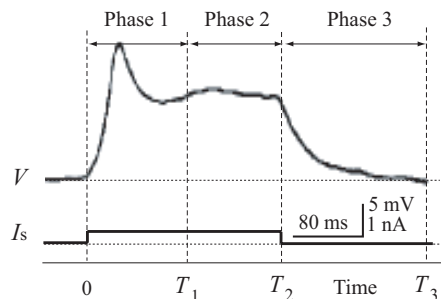
The leak conductance was determined as  $g_{\text{leak}} = 0.045$  mS/cm<sup>2</sup> based on the slope of the line in Figure 8 of Reference [17]. The equilibrium potential of leak ion was set as  $E_{\text{leak}} = -20.1$  mV assuming that the value is near the resting membrane potential.

## 4 Results

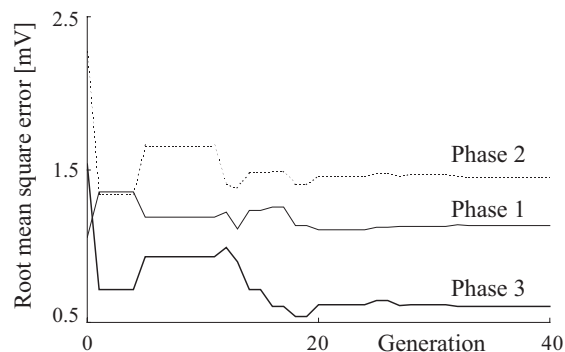
The proposed method was evaluated with the following conditions;  $M = 200$ ,  $G_{\text{max}} = 100$ ,  $\gamma_e = 40$ ,  $\gamma_m = 40$ ,  $N = 2$ ,  $I_1 = 0.4$  nA, and  $I_2 = 1.2$  nA. The data of actual organism in Figure 7 of Reference [18] was used to calculate  $F_m$ . This section shows the estimated results of  $p_n$  ( $n = 1, 2, \dots, 17$ ),  $\bar{g}_{\text{Ca}}$  and  $\bar{g}_{\text{K}}$  by the proposed method.

### 4.1 Estimated parameters

Figure 2 shows the fitness values of the elite individual,  $F_o$ , for 4 different trials. The initial values of the parameters were changed for each trial. From Figure 2, the evolution of the elite fitness was confirmed. Further, in order to confirm the effectiveness of the proposed method in detail, we divided the time variation of the membrane potential change into three phases as shown in Figure 3(a), where Phase 1 ( $0 \leq t < T_1$ ) was the period of overshoot phenomenon, Phase 2 ( $T_1 \leq t < T_2$ ) the stable phase of the membrane potential change, Phase 3 ( $T_2 \leq t < T_3$ ) the decay period after disappearance of current stimuli. The root mean square errors of the actual membrane potential and the elite individual were calculated in each phase. Figure 3(b) shows the results for current stimuli  $I_2$ , when the time threshold were  $T_1 = 40$  ms,  $T_2 = 200$  ms and  $T_3 = 320$  ms. From Figure 3(b), it was confirmed that the error value in Phase 3 was most improved.



(a) Definition of the phase of membrane potential change



(b) Evolved elite fitness in each phase

Figure 3: Details of the elite fitness.

The average values and the standard deviations of the estimated  $\bar{g}_{\text{Ca}}$  and  $\bar{g}_{\text{K}}$  were  $0.133 \pm 0.011$  mS/cm<sup>2</sup> and  $0.195 \pm 0.0021$  mS/cm<sup>2</sup>, respectively. In addition, Figure 4 shows the average values and the standard deviations of  $\tau_x$  and  $x^\infty$  ( $x \in m, h, n$ ) based on the estimated  $p_n$  ( $n = 1, 2, \dots, 17$ ) for 4 different trials. In Figure 4, the black dots indicate the parameter value estimated from the experimental results with the actual organisms [5]. Note that the value of  $h^\infty$  was unreported in Reference [5]. It is confirmed that the estimated parameter values are close to that of the actual organism except  $\tau_n$  in Figure 4 (f).

Figure 5(a) shows the membrane potential changes of actual organism for  $I_s = 0.4, 1.2$  nA [18], (b) the simulation results using the estimated characteristics shown in Figure 4. The overshoot phenomenon, where the membrane potential temporarily drops below the steady-state value after the peak of depolarization, could not be observed for  $I_2 = 1.2$  nA as shown in Figure 5(a). However, this phenomenon was observed in other organisms data for the same current stimuli [19, 20]. Thus, the overshoot phenomenon in Figure 5(b) is considered to be reasonable. From these results, it is confirmed that the model can realize the membrane potential changes similar to that of the actual organism.

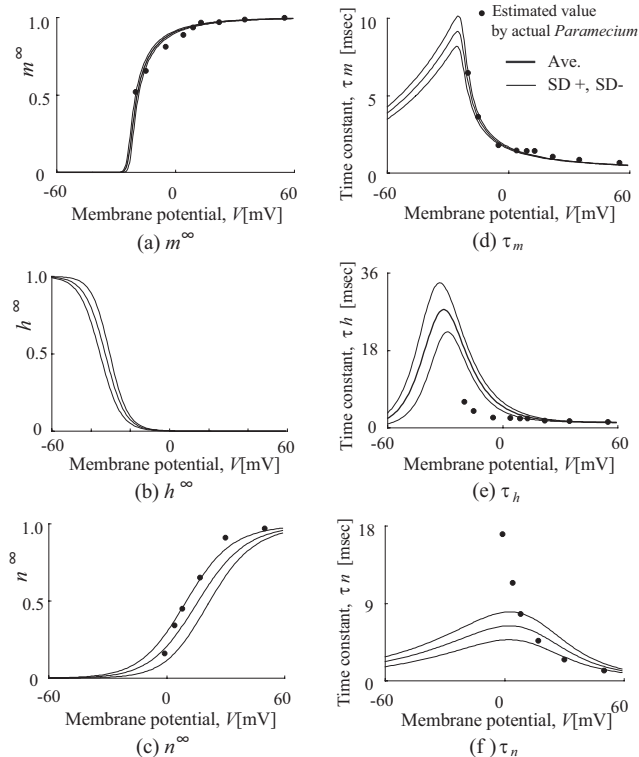


Figure 4: Estimated values of  $x^\infty(V)$  and  $\tau_x(V)$ .

## 4.2 Prediction of the membrane potential change for current stimuli

Finally, the current stimuli simulation was executed using the estimated parameters to examine the predictive ability of *Virtual Paramecium* for various current stimuli not used in the evolutionary computation. Figure 6 shows the simulation results and the membrane potential changes of actual *Paramecium* for  $I = \pm 0.9$  nA.

Figure 6(a) shows the membrane potential change of actual *Paramecium* and the *Virtual Paramecium* for  $I = 0.9$  nA. It is confirmed that the *Virtual Paramecium* is capable of realizing the membrane potential change similar to that of the actual organism. From this result, it can be stated that the estimated parameters by the proposed method are able to realize the membrane potential change is not only  $I = 0.4, 1.2$  nA but also other current values.

Figure 6(b) shows the membrane potential change of actual *Paramecium* and the proposed model for  $I = -0.9$  nA. The proposed model could realize the membrane potential change of actual *Paramecium* qualitatively, but could not realize the overshoot phenomenon. In this paper, we assumed the leak conduc-

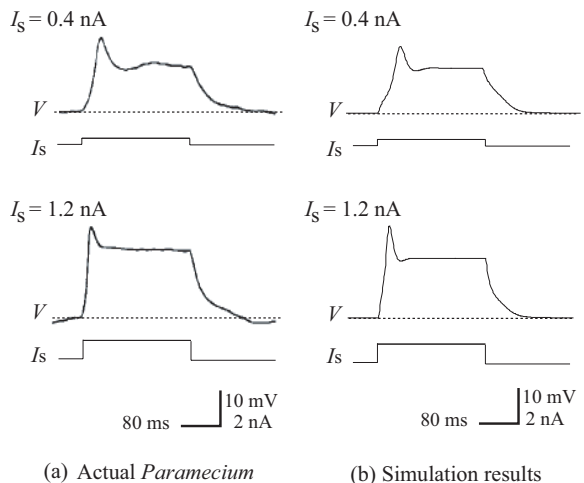


Figure 5: Membrane potentials for current stimuli. (The data of Actual *Paramecium* are revised the figure written by Oami in 1996 [18].)

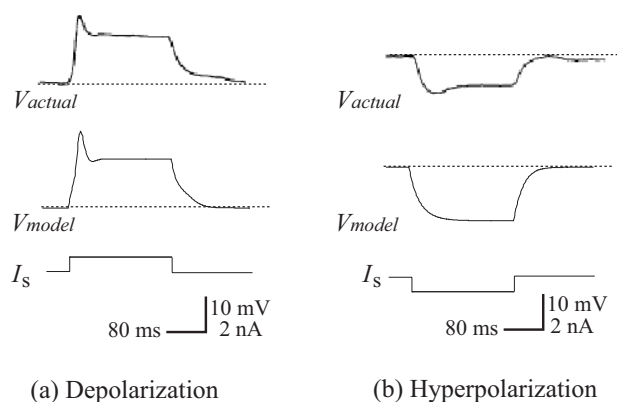


Figure 6: Simulation results for  $I_s = \pm 0.9$  nA. (The data of Actual *Paramecium* are revised the figure written by Oami in 1996 [18].)

tance as a fixed value, but it was reported that its value could be reduced to about 60 % by the hyperpolarization [11]. This detailed mechanism is still not clear, however the hyperpolarization-sensitive  $K^+$  channel is considered as an important factor. In the future works, we plan to introduce the hyperpolarization-sensitive  $K^+$  channel into the proposed model, and analyze the case of Figure 6(b) in more details.

## 5 Summary

In this paper, we proposed an estimation method of the model parameters included in the *Virtual Parame-*

*cium* using a real-coded GA. It was confirmed that the *Virtual Paramecium* can realize the membrane potential changes in the actual *Paramecium* using the estimated parameter values by the proposed method. However, other parameter combinations of parameter values could exist. In the future works, we plan to estimate the parameter values by improving the proposed method.

## Acknowledgements

This work is partially supported by the 21st Century COE Program of JSPS (Japan Society for the Promotion of Science) on *Hyper Human Technology toward the 21st Century Industrial Revolution*.

## References

- [1] R.S. Fearing (1991) : “Control of a Micro-Organism as a Prototype Micro-Robot”, 2nd Int. Symp. on Micromachines and Human Sciences, Nagoya, Japan, Oct. 8-9.
- [2] Akitoshi Itoh (2000) : “Motion Control of Protozoa for Bio-MEMS”, IEEE/ASME Transaction on Mechatronics, Vol. 5, pp. 181.
- [3] N. Ogawa, H. Oku, K. Hashimoto, and M. Ishikawa (2005) : “Microrobotic Visual Control of Motile Cells using High-Speed Tracking System,” *IEEE Transactions of Robotics*, Vol. 21, No. 4, pp. 704–712.
- [4] N. Ogawa, H. Oku, K. Hashimoto, and M. Ishikawa (2006) : “A physical model for galvanotaxis of Paramecium cell,” *Journal of Theoretical Biology*, Vol. 242, Issue 2, pp.314–328.
- [5] A. Hirano, T. Tsuji, N. Takiguchi, and H. Ohtake (2005) : “Modeling of the Membrane Potential Change of *Paramecium* for Mechanical Stimuli,” *Trans. of SICE*, Vol. 41, No. 4, pp. 351–357. (in Japanese)
- [6] A.L.Hodgkin and A.F.Huxley (1952) : “A Quantitative Description of Current and Its Application to Conduction and Excitation in Nerve,” *The Journal of Physiology*, Vol. 117, pp. 500–544.
- [7] A. Hirano, T. Tsuji, N. Takiguchi, and H. Ohtake (2006) : “Simulation for Chemotactic Response of *Paramecium* using *Virtual Paramecium*,” *Trans. of SICE*, Vol. 42, No. 11, pp. 1252–1259. (in Japanese)
- [8] T. Tsuji, K. Hashigami, M. Kaneko, and H. Ohtake (2002) : “Emerging Chemotaxis of Virtual Bacteria using Genetic Algorithm,” *Trans. IEE of Japan*, Vol. 122–C, No. 2. (in Japanese)
- [9] T. Tsuji, A. Sakane, O. Fukuda, M. Kaneko, and Hisao Ohtake (2002) : “Bio-mimetic Control of Mobile Robots Based on a Model of Bacterial Chemotaxis,” *Trans. of the JSME*, Vol. 68 C, No. 673, pp. 171–178. (in Japanese)
- [10] M. Suzuki, T. Tsuji, H. Ohtake (2005) : “A model of motor control of the nematode *C. elegans* with neuronal circuits,” *Artificial Intelligence in Medicine*, 35, pp. 75–86.
- [11] Y. Naitoh (1990) : “Behavior of Unicellular Animals,” University of Tokyo Press. (in Japanese)
- [12] Y. Naito and K. Sugino (1984) : “Ciliary Movement and Its Control in *Paramecium*,” *J. Protozool.*, Vol. 31, pp. 31–40.
- [13] S. Usui (1997) : “Mathematical models of the nervous system,” KYORITSU SHUPPAN CO., LTD., (in Japanese)
- [14] H. Kawakami (2001) : “Dynamics of Biological Rhythmic Phenomena,” CORONA PUBLISHING CO., LTD., (in Japanese)
- [15] H. Ikeno, Y. Kamiyama, and S. Usui (1993) : “Parameter Estimation Method of Ionic Current in a Real Neuron,” *The transactions of the Institute of Electronics, Information and Communication Engineers*, Vol. J76-D-II, No. 5, pp. 1047–1054. (in Japanese)
- [16] L.J Eshleman and J.D Schaffer (1993) : “Real-Coded Genetic Algorithms and Interval-Schemata,” *Foundations of Genetic Algorithms*, Vol. 2, pp. 187–202.
- [17] Y. Naitoh (1986) : “New Physiological Science Outline 1 Physiology of Excitable Membrane (Watanabe, Yamagishi edition),” Igaku-Shoin, pp. 242–257. (in Japanese)
- [18] K. Oami (1996) : “Membrane potential responses controlling chemodispersal of *Paramecium caudatum* from quinine, *J Comp Physiol A* 178, 307–316.
- [19] H. MACHEMER and A. OGURA (1979) : “IONIC CONDUCTANCES OF MEMBRANES IN CILIATED AND DECILIATED *PARAMECIUM*,” *J. Physiol.*, 296, pp. 49–60.
- [20] R.D. HINRICHSEN and Y. SAIMI (1984) : “A MUTATION THAT ALTERS PROPERTIES OF THE CALCIUM CHANNEL IN *PARAMECIUM TETRAURELIA*,” *J. Physiol.*, 351, pp. 397–410.